Indium Tin Oxides: Promising Plasmonic Material Supporting Recent Advances in Biosensors

Sukla Rajak

M.U.C.Women's College, Bardhaman, West Bengal 713104, India

E-mail: sukla.phy@gmail.com

(Received: August 13, 2024; Revised: September 12, 2024; Accepted: October 01, 2024; Published: March 30, 2025)

Abstract: Transparent conducting oxides (TCOs) have emerged as promising alternative materials to conventional metals for plasmonic applications in the near-infrared (NIR) and telecommunication frequency regions. The optical and electrical properties of TCOs make them suitable substitutes for metals in plasmonic and metamaterial (MM) devices based on Surface Plasmon Resonance (SPR). SPR characteristics in TCOs strongly depend on material thickness and the angle of incident electromagnetic radiation. This study investigates the optical and electrical properties of Indium Tin Oxide (ITO) for its potential applications as a plasmonic material in optoelectronics and biosensors.

Keywords: TCO, Surface Plasmon Resonance (SPR), Meta-Materials, Surface Plasmon Polariton (SPP), Full Width Half Maximum (FWHM), Sensors, Fano resonance.

I Introduction

Recent study of optoelectronics and metamaterial (MM) (1; 2) research have some limitations of applications due to the use of plasmonic materials, based on metals. In the visible and near infrared region metals like gold and silver peruse high losses (3; 4). They have large real negative permittivity values in this optical region and their optical properties cannot be tuned. In the visible region they possess high losses also (3). To overcome these limitations while using metal based plasmonic materials / meta-materials (MMs) and optoelectronic devices recent researchers put on focus on using semiconductors as building blocks. Heavily doped semiconductors having wide band gap like Indium tin oxides (ITO) have small negative real permittivity in the NIR region (5; 6; 7; 8) and the optical losses are also small in this region. With the increment of thickness of indium tin oxide film on BK7 glass, Surface Plasmon generates without interference from band-to-band transitions in the conducting thin films which faces complications in metals like Ag and Au. Due to these factors ITO can be a good alternative to metals in Plasmonic applications in NIR range (9; 10; 11; 12). These types of TCOs may be applied in Surface Plasmon Polariton waveguides to meta-materials with hyperbolic dispersion and epsilon-near-zero (ENZ) materials (13; 14; 15) in Near infrared region, optoelectronic devices, and biosensors.

Metals are the good choice of plasmonic devices for supporting collective oscillations of free electrons and for focusing the light to nanoscale. Due to interband electronic transitions in metals (16), they suffered from high optical losses in optical and telecommunication ranges in which plasmonic devices are operated. Conventional metals have negative real permittivity of large value which also limits the performance of plasmonic devices in near infrared and telecommunication wavelength of 1.55µm. High optical losses and large negative real permittivity limits the plasmonic devices using metals.

Whereas TCO s having carrier concentration higher than 10^{20} cm^{-3} behaves like metals in the NIR region (17). When the carrier concentration in the TCOs exceeds the Mott critical density $10^{18} - 10^{19}$ cm^{-3} (6), a semiconductor may transit to metal and the conduction band shifts the onset of band edge absorption in the ultraviolet region (Burstein- Moss shift) (6; 18; 19) due to the filled state by the free electrons. By controlling and optimising some fabrication condition such as doping concentration (20),

dopant type, deposition temperature and pressure, TCOs can have critical optical properties which is suitable for plasmonic applications. Having large plasma frequency TCOs exhibit Drude metal like optical properties (21). According to Drude response (22) of such degenerately doped semiconductors material's (23; 18; 24) complex electrical permittivity or dielectric function (ε) is described by the equation

$$\varepsilon = \varepsilon^{'} + i\varepsilon^{''} = \varepsilon_{\infty} - \frac{{\omega_p}^2}{\omega(\omega + i\gamma)} \tag{1}$$

(15), where ε_{∞} is high frequency dielectric constant arises due to the screening effect of bound electrons in the material, $\varepsilon^{'}$ is the real part of complex dielectric function which describes the strength of the polarization induced by an external electric field, $\varepsilon^{''}$ is the imaginary part of complex dielectric function and γ is the Drude relaxation rate or damping coefficient of the free carriers. This describes the losses encountered in polarizing material. So for having negative real permittivity in the NIR and telecommunication range the value of ω_p must be large and ε_{∞} must be small and for lower optical loss γ value should be small (15). TCOs can have losses one fourth of that happened in case of Ag in NIR region (3). The carrier concentration has large dependence on the thickness of the TCO film (25; 26; 27; 28; 29; 30; 31).

In ITO, tin acts as a cationic dopant in the in the In_2O_3 lattice and substitute on the indium sites to bind with the interstitial oxygen. The ITO films have wide band gap (> 3 eV) becoming highly transmitting in the NIR range and hence is preferred in most of the applications. Thus, the dopant Sn improve the conductivity of In_2O_3. Indium tin oxide has good electrical conductivity, low resistivity $\sim 10^{-4}\Omega$ cm and high transmittance of $\sim 90\%$ when the ITO film is coated on glass substrate. Having this property, among all the TCOs, Indium tin oxide (ITO) shows the potential for good alternatives to metals in optoelectronic devices and solar cells based on surface Plasmon resonance in the NIR and telecommunication region of 1.55 µm. The existence of both bulk and surface Plasmon polariton (SPPs) in indium tin oxide are well demonstrated experimentally by Rhodes et al (12; 32).

Surface Plasmon Resonance (SPR) is an optical phenomenon occurs in the materials due to interaction of charges with the incident p-polarised light. By this phenomenon, the change of the refractive index at the dielectric/metal interface can be detected. The reflected light's intensity drops to its lowest point at a specific angle or wavelength, marked by a sharp decline in the SPR curve.

Surface Plasmon resonance is dependent on energy of incident radiation, thickness of metal or metal oxide film and angle of incidence and described by the three phase Kretshmann (substrate/overlayer/ambient) model (32). This Kretshmann representation is sensitive for thin film, for larger thicknesses this structure gradually weakens, in consonance with theory. No other collective excitations are observed.

In this paper theoretical investigations on SPP propagation in TCO thin films (ITO) at the IR and NIR wavelength region is reported and it is also reported that ITO can be a substitute to metal in optoelectronic and biosensors. For the study four different thick ITO coated on BK7 glass slides are considered and comparative analysis supported by MATLAB simulations is presented. The optimised thickness and the angle of incidence of the light and thickness of the ITO film suitable for sensors application is also investigated.

II Materials and methods

Polarisation is the property of certain electromagnetic radiations in which the direction and magnitude of the vibrating electric field are related in a specified way. The electric field vector has two components one is normal to the interface and one is tangential. The interaction between electromagnetic waves with materials is described by the method of polarisation. The polarisation of waves in material is

defined by the complex dielectric function of that material. According to classical Drude theory, the complex electrical permittivity or dielectric function is defined as

$$\varepsilon = \varepsilon^{'} + i\varepsilon^{''} = \varepsilon_{\infty} - \frac{{\omega_p}^2}{\omega(\omega + i\gamma)} \tag{2}$$

where, ε_{∞} is the high frequency dielectric constant, γ is damping coefficient of free electrons and ω_p is plasma frequency.

The high-frequency dielectric constant ε_{∞} originates from the bound electrons' screening effect in the material, whereas the damping coefficient γ characterizes free electron scattering and optical losses. To minimize losses, materials should possess a small γ value. Achieving negative permittivity (ε) in the optical range requires materials with a high plasma frequency ω_p and a low ε_{∞} value. A large ω_p leads to Drude-like metallic optical properties. The plasma frequency is defined as:

$$\omega_p = \sqrt{\frac{ne^2}{\varepsilon_0 m^*}} \tag{3}$$

where n represents the charge carrier density, e is the electron charge, m^* denotes the effective mass, and ε_0 is the vacuum permittivity. By increasing the carrier density (through doping, for instance), materials can exhibit metallic characteristics, making them suitable for plasmonic applications. Several special methods have been developed by Scientists to excite the Surface Plasmon Polariton. Kretschmann configuration is the most widespread geometry. In this geometry, the Plasmon can be excited on the prism surface by p-polarized light under the condition of total internal reflection (TIR) and by this time evanescent wave to be released and decayed exponentially.

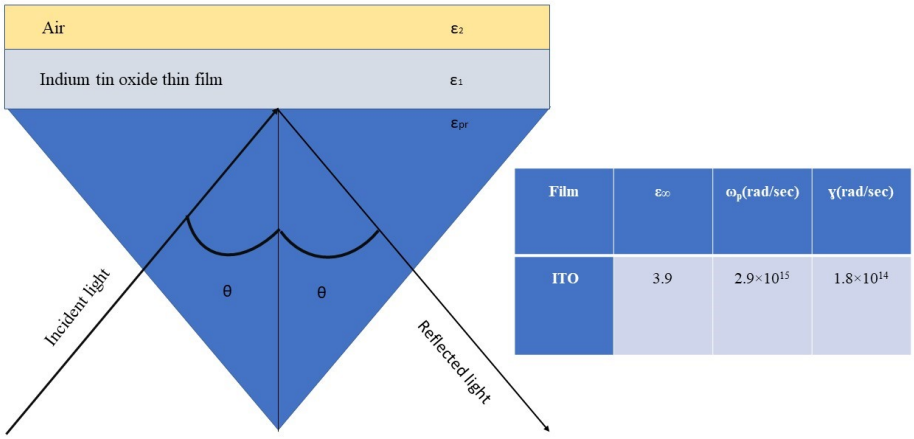

Film	ε_{∞}	ω_p(rad/sec)	γ(rad/sec)
ITO	3.9	2.9×10^{15}	1.8×10^{14}

Figure 1: Kretschmann configuration in three-layer model.(33)

The electric field of the light incident on the prism has the form of

$$E = E_0 e^{i(k\cdot r - \omega t)} \tag{4}$$

where, E_0 is the amplitude of the applied electric field, and ω is the frequency of the applied electric field. The component of the incident electromagnetic radiation has wave vector (k_i). It has wave

vector $k_i = (k_x, 0, k_z)$ and angular frequency ω. Electromagnetic wave should obey the Maxwell's electromagnetic equation. To satisfy these equations, the condition should be satisfied is, $k_i = \frac{\omega}{c} n_p \sin\theta$, where c is the velocity of light. k_i can be expressed by the equation

$$k_i = \frac{2\pi}{\lambda} n_p \sin\theta \tag{5}$$

Where n_p is refractive index of prism, θ is the Attenuated total reflection angle (SPR angle) and λ is the wavelength of the polarized light. And the wave vector of the generated Plasmon mode $k_p = \frac{2\pi}{\lambda}\sqrt{\frac{\varepsilon_1\varepsilon_2}{\varepsilon_1+\varepsilon_2}}$ where (ε_1) is the dielectric constant for metal oxide thin film and (ε_2) is the dielectric constant of dielectric medium air. At the critical condition when the wave vector k_i of the incident electromagnetic light is equal to the wave vector k_p of the Plasmon mode then surface Plasmon resonance occurred and a decrease in the intensity of the reflected light occurs. There is a phase difference between the surface Plasmon mode with respect to incident electromagnetic wave and this phase difference leads to the phenomenon of destructive interference. Furthermore, the minimum intensity of the reflected light is shown as a curve which is called the SPR curve.

In the Kretschmann geometry (shown in Fig. 1), the total reflectance R is determined by considering the field reflections at both interfaces: the prism-metal oxide boundary and the metal oxide-air boundary. Denoting the field reflection coefficient at the prism-metal oxide interface as r_{p1} and at the metal oxide-air interface as r_{12}, these reflection coefficients can be calculated using the following expressions:

$$r_{p1} = \frac{\varepsilon_1 k_{z0} - \varepsilon_0 k_{z1}}{\varepsilon_1 k_{z0} + \varepsilon_0 k_{z1}} \tag{6}$$

$$r_{12} = \frac{\varepsilon_2 k_{z1} - \varepsilon_1 k_{z2}}{\varepsilon_2 k_{z1} + \varepsilon_1 k_{z2}} \tag{7}$$

where ε_1 is the dielectric constant of Indium tin oxide layer and ε_2 is the dielectric constant of air.

In this three-layer model, according to Airy equation, the field reflectance r_{p12} is defined as,

$$r_{p12} = \frac{r_{p1} + r_{12} e^{2ik_{z1}d_1}}{1 + r_{p1} r_{12} e^{2ik_{z1}d_1}} \tag{8}$$

where, in the phase term, k_{z1} is the z component of the wave vector in medium 1 i.e. in CMO (Complementary Metal Oxide like Tin Oxides) layer and d_1 is the thickness of the film.

Then the reflectance is $R = |r_{p12}|^2$,

In this work wave no ranges from 500 cm^{-1} to 10000 cm^{-1}, incident angle from 42° to 69°.

III Results and discussion

For the study of behaviour of surface plasmon polariton three phase Kretschmann configuration (prism /metal oxide layer (medium 1) /air (medium 2)) model is taken. The layer wise Kretschmann configuration is described in Fig 1.

Indium tin oxides are often opaque and transparent depending upon the angle of incidence and thickness of the film. ITO have optimized constraints to give resonance to excitations by external light and also to dual peak resonance.

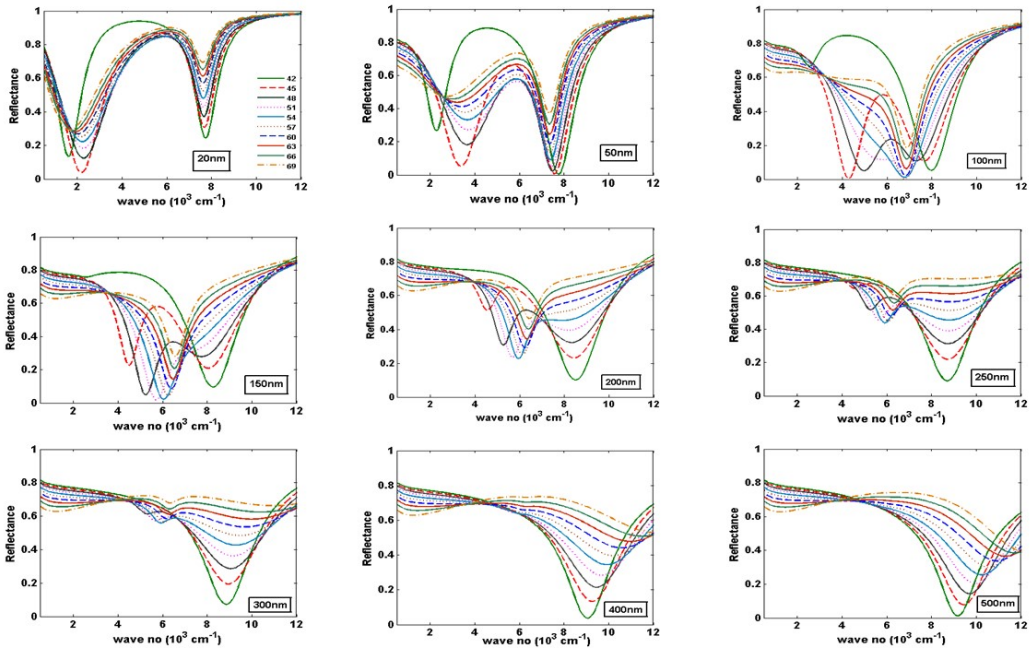

Figure 2: Reflectance vs. wave number curves for different thicknesses of ITO film from 20 nm to 500nm, with θ varying from 42° to 69° as shown in the legend.

Figure 2 demonstrates the surface plasmon coupling phenomenon in ITO films of varying thicknesses using Kretschmann geometry. The reflection spectra clearly show distinct surface plasmon polariton (SPP) resonances, evidenced by sharp reflectance minima for each film thickness.

For films below 100 nm thickness, the probability of electron excitation by incident radiation (at 45° angle) is significantly higher compared to thicker ITO layers. Our analysis identifies 60 nm as the optimal thickness, yielding the lowest reflectance in these plasmonic studies.

Figure 2 depicted the variation of reflectance when the reflected light is detected from metal oxide layer with wave no of the incident light beam for different incident angle from 42° to 69° in step of 1° for different thick metal oxide film. For 20 nm Indium tin oxide layer, Surface Plasmon resonance occurs at two different positions of wave no of incident radiation for the angle region of 42° to 69°. When the exciting electromagnetic radiation incident at 42° incident angle first resonance occurs at 1591 cm^{-1} of wave no and second resonance at 7745 cm^{-1} of angular frequency with minimum reflectance 0.243. For 54° the surface plasmon resonance occurs at 2228 cm^{-1} with minimum reflection of 21.03% and at 7639 cm^{-1} with minimum reflectance 46.18%. For 50nm thick ITO the reflectance become minimum for first position at 2281 cm^{-1} and for second position at 7745 cm^{-1} for 42° incident angles where for 54° surface resonance position occurs at 7427cm^{-1}.

From the variation of reflectance curve with the different thickness for 60 nm thick ITO metal oxide responds to surface plasmon resonance with the minimum reflectance 0.18% at 7586 cm^{-1}. For 150nm thick metal oxide film coated on the prism the reflectance profile had dual dips with two minimum position one is 4509 cm^{-1} with reflectance 22.66% and another is at 8064 cm^{-1} transferred position from 7957 cm^{-1} with reflectance 4.229% at 45° angle of incidence to the minimum reflectance position 6578 cm^{-1} with reflectance 27.93% when the incident light incidents on the configuration at 69° incident angle. The minimum reflectance values for searching the resonant thickness according to thickness variation is provided in the table given below.

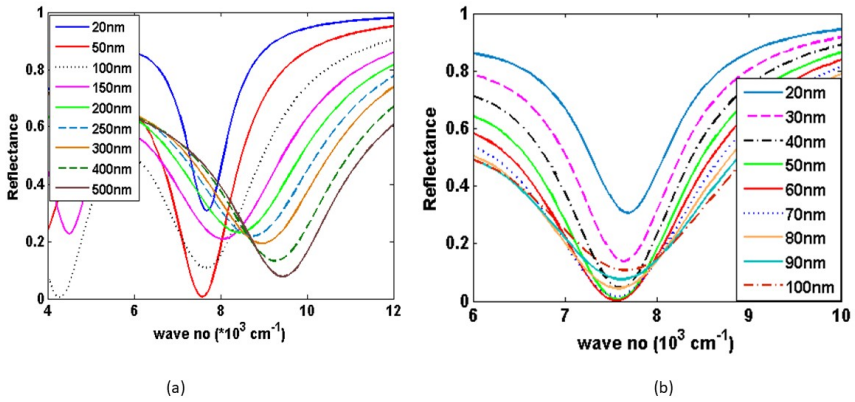

Figure 3: Reflectance vs. wave number curves for different thicknesses of ITO film at the incident angle 45°

Table 1: Reflectance values for different thicknesses of ITO film

Thickness(nm)	**Wave no (cm^{-1})**	**Reflectance**
20	7692	0.3067
30	7639	0.1382
40	7586	0.04639
50	7586	0.00647
60	7586	0.001813
70	7586	0.01764
80	7586	0.0444
90	7639	0.07625
100	7692	0.1076

With the increment of thickness, it is noticed that for 90nm thick ITO when excited with the exciting light of NIR region shows surface plasmon resonance at 6950cm^{-1} with the minimum reflectance of 0.03% and also 130nm thick ITO response to SPR resonance at 6260cm^{-1} with reflectivity 0.031%. So reflectivity gets minimum for two thickness one for 90nm and 130nm when the exciting light incident on the Kretschmann configuration at 55° angle.

In case of selection of film thickness minimum reflectance for surface plasmon resonance and full width half maximum (FWHM) both are to be considered. FWHM has been plotted in angular interrogation in Fig 4. It can be seen that for 50 nm thick indium tin oxide film at first FWHM increases to a peak value of 1857cm^{-1} with the increment of incident angle at 47° and then decreases to value 1751 cm^{-1} for again increment of the incident angle upto 54° incident angle. When the thickness of the metal oxide film (ITO) taken is 60nm then FWHM gradually increases from 1910cm^{-1} to 2387cm^{-1} for 42° to 53° incident angle of the exciting radiation.

Maximum and minimum value of FWHM signifies how much the metal oxide films supports the coupling for SPP resonance. On the other hand FWHM first increases to a value 2069 cm^{-1} at 48° and then decrease to a value 1910cm^{-1} of wave number for 54° incident angle. From these values it can be concluded that lower the value of FWHM defines the better performance of the device.

The detection accuracy is quantitatively defined as the reciprocal of the full-width-at-half-maximum (FWHM), establishing that narrower resonance widths enable higher sensing precision.

From a performance perspective, minimizing the FWHM is crucial as it directly enhances detection accuracy - a critical parameter for sensor applications. Our results demonstrate that a 50 nm ITO film exhibits this desirable characteristic, showing significantly reduced FWHM compared to other thicknesses.

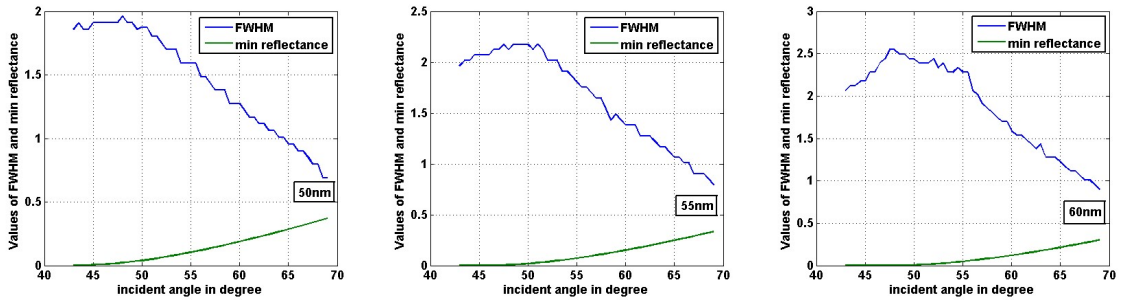

Figure 4: FWHM and minimum reflectance position vs angle of incidence of exciting light of 1.55 micron wavelength.

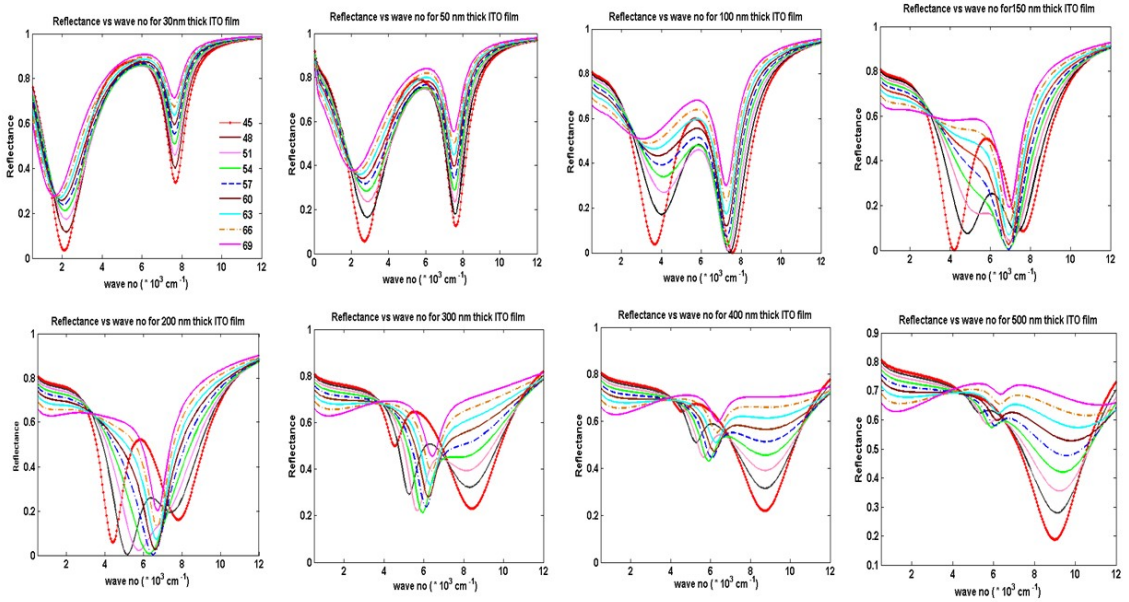

Figure 5: Reflectance vs. wave number curves for different thicknesses of ITO film at the incident angle 45° when the metal oxide layer is excited by light of wavelength 2.5 µm range.

The variation of Surface plasmon polariton resonance curves with the frequency and the incident angle of the exciting light of 2.5-micron wavelength range is plotted in the Fig 5. Different subsections of the Fig 5 describe the variation of surface plasmon resonance with different thickness of the indium tin oxides. From the theoretical data it is found that the angle of incidence at resonance condition is 42°.

The variation of reflectance with the wave number of the incident different thickness of Indium tin oxide at an angle 45° when the incident light is in the range of 2.5micron shows that the configuration

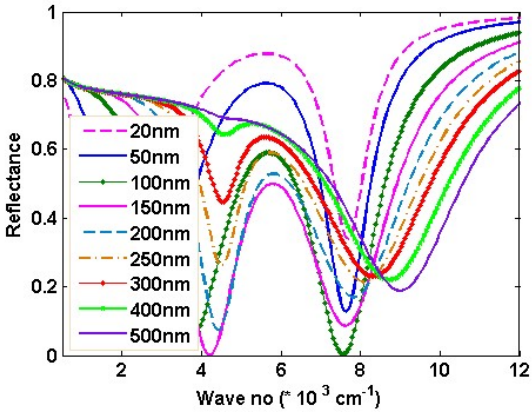

Figure 6: Reflectance vs. wave number curves for incremental thicknesses of ITO film at the incident angle 45° when the metal oxide layer is excited by light of wavelength 2.5 µm range.

responses to surface plasmon polarisation for the Indium tin oxide of thickness between 50nm to 150nm where the angle variation is taken from 42° to 69°.

From the Reflectance variation profile with respect to the thickness of the Indium tin oxide in the wavelength region 2.5 µm, it is noticed that the minimum reflectance is possible for 90nm thick Indium tin oxide and the numerical data is provided in the table given below.

Table 2: Reflectance values for different thicknesses of ITO film at 2.5 µm wavelength

Thickness(nm)	**Wave no(cm^{-1})**	**Reflectance**
50	7639	0.126
60	7586	0.04621
70	7586	0.02848
80	7586	0.00727
90	7586	0.0005583
100	7586	0.00371
110	7586	0.01376
120	7586	0.02848
130	7586	0.04621
140	7586	0.06574
150	7639	0.08555

30 nm thick indium tin oxide film shows two minimum reflectivity position at 2122 cm^{-1} and 7692 cm^{-1} (0.954 eV) in this frequency range. The secondary reflectance minimum at 7692 cm^{-1} (0.954 eV) indicates screened bulk plasmon polariton (SBPP) resonance, appearing at slightly lower energy than the theoretical prediction $\omega_{ps} = \omega_p/\sqrt{\varepsilon_\infty} = 7771\,cm^{-1}$ (0.964 eV). While the SBPP frequency remains constant with increasing angle θ, the reflectivity enhancement suggests reduced light absorption, as visible in the spectral profile evolution (red to pink curves).

For 100 nm ITO films, the reflectivity minimum between 6000–8000 cm^{-1} nearly reaches zero, demonstrating efficient plasmon coupling. Thicker films exhibit altered SBPP behavior: at 150 nm, the resonance shifts to higher energies (7639 cm^{-1} at 45°) and lower energies (7056 cm^{-1} at 54°), eventually becoming angle-independent at larger θ - characteristic of SPP resonance.

Analysis of reflectance spectra reveals optimal SPP coupling occurs for 200 nm thickness. For 500 nm

films, plasmon excitation only persists at angles below 48° with significantly reduced efficiency, while higher angles show negligible light-plasmon coupling.

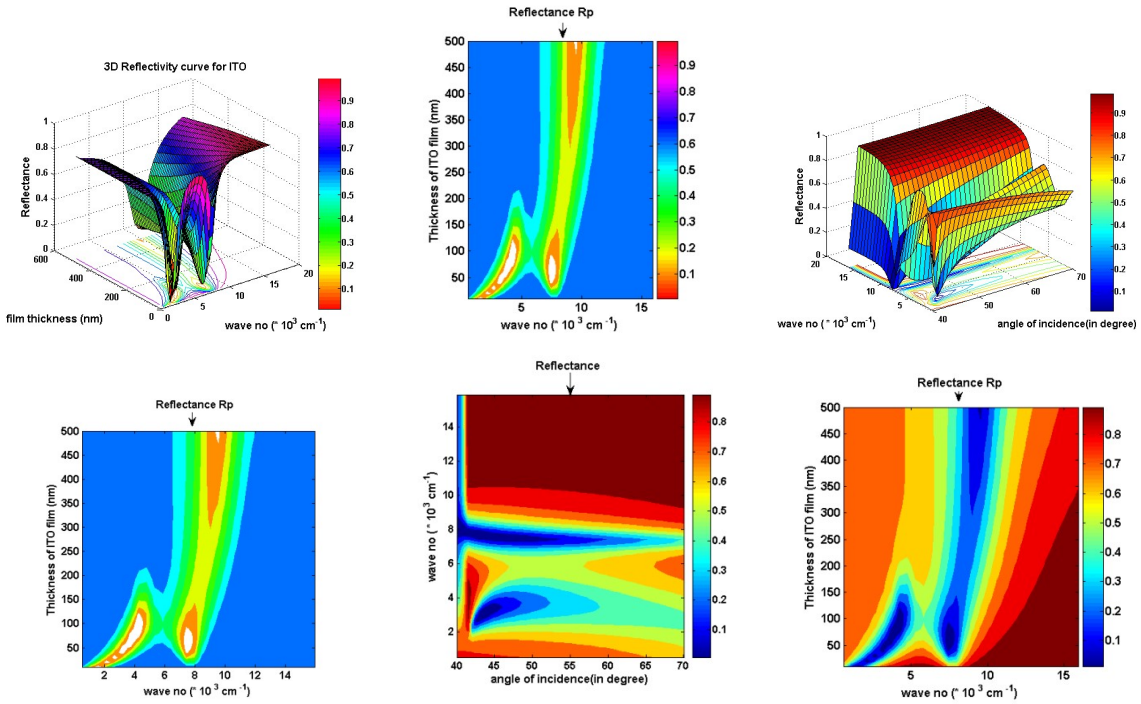

Figure 7: Three-dimensional variation of reflectance curve with the incident angle and thickness of the indium tin oxide layer.

Three-dimensional variation of Reflectance with the incident angle of the exciting radiation and thickness of the ITO thin film is described in Fig. 7. These figures predict dual peak resonance of ITO in both 1.55 µm and 2.5 µm wavelength range. The type of resonance is called Fano resonance shown in ITO.

III.a Sensor performance: related sensitivity issues

Indium tin oxide (ITO) demonstrates promising plasmonic properties for sensing applications. Our theoretical investigation employs a 3-phase configuration with air as reference to analyze various gaseous samples. The sensing mechanism relies on monitoring spectral shifts of the reflectance minimum, which correlates with the sample's refractive index. The system sensitivity is quantitatively determined by the resonant wave number variation per unit refractive index change.

Figures 8(a) and 8(b) present reflectance spectra for different samples (with refractive indices specified in the legend) across 1.55–2.5 μm wavelength ranges. The resonance shifts appear minimal due to small wave number variations. The sensitivity is formally defined as $\Delta\tilde{\nu}/\Delta n$, where $\Delta\tilde{\nu}$ represents the resonant wave number shift and Δn denotes the refractive index change between samples.

We have theoretically studied sensing of different gaseous samples taking air as reference using the proposed structure. We investigated the sensitivity of 60nm thick ITO in the 1.55-micron frequency range and 90nm thick ITO film in 2.5-micron frequency range. The shift of dip in the reflection spectrum is used to detect the sample in terms of refractive index. Zoomed insets of the corresponding dips are used in order to calculate sensitivity. Fig. 8 shows that resonance wave number shifts to higher value when sample refractive index increases. This implies that measurements with ITO thin film

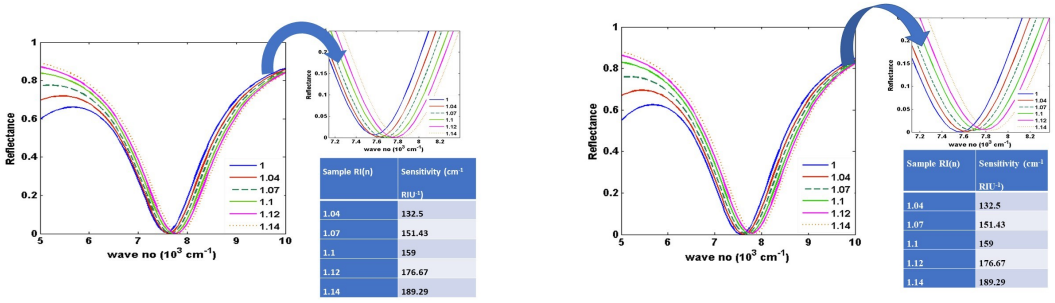

Figure 8: Sensing of gaseous samples using ITO film in (a) 1.55 micron (b) 2.5-micron incident frequency range

layer is more sensitive and can be used as sensing materials in case of sensors. One of the prospective approaches to further improving the sensing technique involves both detection accuracy and sensitivity.

IV Conclusions

Indium tin oxide can be used as a good substitute to metals in the present application exploiting Surface Plasmon Resonance feature. The metal oxide in both IR and near IR region can provide sensing properties and can be used in bio sensors and geo sensors. In both the frequency range ITO shows dual peak Fano resonance and supports it's promising application in the field of Sensors in both the frequency range of IR and NIR.

References

[1] V. Veselago. The electrodynamics of substances with simultaneously negative values of and . *Physics-Uspekhi*, 10:509–514, 1968.

[2] J. Pendry. Negative refraction makes a perfect lens. *Physical Review Letters*, 85:3966–3969, 2000.

[3] P. R. West, S. Ishii, G. V. Naik, N. K. Emani, V. M. Shalaev, and A. Boltasseva. Searching for better plasmonic materials. *Laser & Photonics Reviews*, 4:795–808, 2010.

[4] A. Boltasseva and H. A. Atwater. Low-loss plasmonic metamaterials. *Science*, 331:290, 2011.

[5] K. H. Kim, K. C. Park, and D. Y. Ma. Electrical and optical properties of aluminum-doped zno thin films deposited by rf magnetron sputtering. *Journal of Applied Physics*, 81:7764–7772, 1997.

[6] I. Hamberg and C. G. Granqvist. Evaporated sn-doped in_2o_3 films: Basic optical properties and applications to energy-efficient windows. *Journal of Applied Physics*, 60:R123–R159, 1986.

[7] A. J. Hoffman, L. Alekseyev, S. S. Howard, K. J. Franz, D. Wasserman, V. A. Podolskiy, E. E. Narimanov, D. L. Sivco, and C. Gmachl. Negative refraction in semiconductor metamaterials. *Nature Materials*, 6:946–950, 2007.

[8] J. A. Schuller, R. Zia, T. Taubner, and M. L. Brongersma. Dielectric metamaterials based on electric and magnetic resonances of silicon carbide particles. *Physical Review Letters*, 99:107401, 2007.

[9] P. F. Robusto and R. Braunstein. Optical absorption in indium tin oxide films. *Physica Status Solidi (a)*, 119:155–168, 1990.

[10] M. Y. C. Xu, M. Z. Alam, A. J. Zilkie, K. Zeaiter, and J. S. Aitchison. Optical characterization of indium tin oxide for plasmonic applications. In *Conference on Lasers and Electro-Optics/Quantum Electronics and Laser Science Conference*, pages 2135–2136. IEEE, 2008.

[11] F. Michelotti, L. Dominici, E. Descrovi, N. Danz, and F. Menchini. Thickness dependence of surface plasmon polariton dispersion in transparent conducting oxide films at 1.55 m. *Optics Letters*, 34:839–841, 2009.

[12] C. Rhodes, S. Franzen, J. P. Maria, M. Losego, D. N. Leonard, B. Laughlin, G. Duscher, and S. Weibel. Surface plasmon resonance in conducting metal oxides. *Journal of Applied Physics*, 100:054905, 2006.

[13] M. Silveirinha and N. Engheta. Tunneling of electromagnetic energy through subwavelength channels and bends using -near-zero materials. *Physical Review Letters*, 97:157403, 2006.

[14] N. Engheta. Circuits with light at nanoscales: Optical nanocircuits inspired by metamaterials. *Science*, 317:1698–1702, 2007.

[15] G. V. Naik and A. Boltasseva. A comparative study of semiconductor-based plasmonic metamaterials. *Metamaterials*, 5:1–7, 2011.

[16] W. Cai and V. Shalaev. *Optical Metamaterials: Fundamentals and Applications*. Springer, 2009.

[17] G. V. Naik, J. Kim, and A. Boltasseva. Oxides and nitrides as alternative plasmonic materials in the optical range. *Optical Materials Express*, 1:1090–1099, 2011.

[18] Z. C. Jin, I. Hamberg, and C. G. Granqvist. Optical properties of sputter-deposited zno:al thin films. *Journal of Applied Physics*, 64:5117, 1988.

[19] B. E. Sernelius, K. F. Berggren, Z. C. Jin, I. Hamberg, and C. G. Granqvist. Band-gap tailoring of zno by means of heavy al doping. *Physical Review B*, 37:10244, 1988.

[20] H. Fujiwara and M. Kondo. Effects of carrier concentration on the dielectric function of zno:ga and in_2o_3:sn studied by spectroscopic ellipsometry: Analysis of free-carrier and band-edge absorption. *Physical Review B*, 71:075109, 2005.

[21] G. V. Naik and A. Boltasseva. Semiconductors for plasmonics and metamaterials. *Physica Status Solidi (RRL)*, 4:295–297, 2010.

[22] A. Solieman and M. A. Aegerter. Modeling of optical and electrical properties of in_2o_3:sn coatings made by various techniques. *Thin Solid Films*, 502:205–211, 2006.

[23] I. Hamberg and C. G. Granqvist. Band gap widening in heavily sn-doped in_2o_3. *Journal of Applied Physics*, 60:R123, 1986.

[24] S. Chatterjee, R. Mukherjee, S. Chandra, A. R. Maity, S. Kumar, and P. S. Maji. Harnessing tamm-plasmon polaritons in cantor sequence photonic quasicrystals for enhanced cancer cell detection. *Plasmonics*, pages 10–1007, 2024.

[25] Y. Shigesato, S. Takaki, and T. Haranou. Study on the electrical and optical properties of sn-doped in_2o_3 films deposited by dc magnetron sputtering. *Applied Surface Science*, 48:269–276, 1991.

[26] T. Minami, H. Sato, H. Nanto, and S. Takata. Highly conductive and transparent silicon-doped in_2o_3 films prepared by rf magnetron sputtering. *Japanese Journal of Applied Physics*, 24:L781–L784, 1985.

[27] Y. Qu, T. A. Gessert, K. Ramanathan, R. G. Dhere, R. Noufi, and T. J. Coutts. Indium tin oxide films prepared by radio frequency magnetron sputtering method at room temperature. *Journal of Vacuum Science & Technology A*, 11:996–1001, 1993.

[28] B. H. Choi, H. B. Im, J. S. Song, and K. H. Yoon. Electrical and optical properties of indium tin oxide films deposited by activated reactive evaporation. *Thin Solid Films*, 193:712–720, 1990.

[29] J. Hu and R. G. Gordon. Atmospheric pressure chemical vapor deposition of gallium doped zinc oxide thin films from diethyl zinc, water, and triethyl gallium. *Journal of Applied Physics*, 72:5381–5392, 1992.

[30] S. Major, A. Banerjee, and K. L. Chopra. Highly transparent and conducting indium-doped zinc oxide films by spray pyrolysis. *Thin Solid Films*, 125:179–185, 1985.

[31] U. Chowdhury, P. Mandi, R. Mukherjee, S. Chandra, S. Sutradhar, S. Kumar, and P. S. Maji. Dual self-referenced refractive index sensor utilizing tamm plasmons in photonic quasicrystal for multistage malaria parasite detection. *Plasmonics*, pages 10–1007, 2024.

[32] C. Rhodes, M. Cerruti, A. Efremenko, M. Losego, D. E. Aspnes, J. P. Maria, and S. Franzen. Dependence of plasmon polaritons on the electron density in doped zinc oxide. *Journal of Applied Physics*, 103:093108, 2008.

[33] S. Rajak. Recent advances in sensors applications using azo and gzo as plasmonic material in ir and nir frequency region. *Natural Sciences and Applied Technology*, pages 1–11, 2024.